Inter-Landau level magnetoexcitons in bilayer graphene

Judit Sári[1] and Csaba Tőke[2]
[1]*Institute of Physics, University of Pécs, H-7624 Pécs, Hungary and*
[2]*BME-MTA Exotic Quantum Phases "Lendulet" Research Group,*
Budapest Univ. of Technology and Economics, Institute of Physics, Budafoki ut 8., H-1111 Budapest, Hungary
(Dated: September 5, 2012)

If bilayer graphene is placed in a high perpendicular magnetic field, several quantum Hall plateaus are observed at low enough temperatures. Of these, the $\sigma_{xy} = 4ne^2/h$ sequence ($n \neq 0$) is explained by standard Landau quantization, while the other integer plateaus arise due to interactions. The low-energy excitations in both cases are magnetoexcitons, whose dispersion relation depends on single- and many-body effects in a complicated manner. Analyzing the magnetoexciton modes in bilayer graphene, we find that the mixing of different Landau level transitions not only renormalizes them, but essentially changes their spectra and orbital character at finite wave length. These predictions can be probed in inelastic light scattering experiments.

PACS numbers: 71.35.Ji, 71.70.Di, 71.70.Gm

I. INTRODUCTION

Bilayer graphene,[1] two coupled hexagonal lattices of carbon atoms in the Bernal stacking[2] of graphite, is a two-dimensional zero-gap semiconductor with chiral charge carriers with Berry's phase 2π, having a roughly parabolic dispersion at low energies about the corners of the hexagonal first Brillouin zone.[3] These facts are testified by its unusual integer quantum Hall effect[4,5] (IQHE), featuring a double step in the ladder of the Hall conductance in a strong perpendicular magnetic field $B_\perp$, first observed by Novoselov *et al.*[1] This double step, $8e^2/h$ instead of the common $4e^2/h$ for spin and valley degenerate Landau levels, is due to the degeneracy of the $n = 0, 1$ Landau orbitals.[6–8] The gap at the integer quantum Hall effect at filling factor $\nu = \rho hc/eB_\perp = \pm 4, \pm 8$ have been recently measured with great accuracy,[9] and the excitations of the IQHE states in the long wavelength limit have also been observed by infrared absorption[10] and Raman spectrocopy.[11] Further broken symmetry states have been observed[12–15] in the central Landau band at $\nu = 0, \pm 1, \pm 2$ and ± 3, and by careful tilted-field measurements it has been shown that they arise predominantly from many-body effects, i.e., from quantum Hall ferromagnetism (QHF).[16] Quantum Hall states with broken symmetry have also been found in the $n = -2$ Landau level[17], and there is also some evidence for a fractional quantum Hall plateau.

The eightfold degeneracy of the central group of Landau levels is at best approximate, because the Zeeman energy is unavoidably present. While the latter is rather small on the characteristic scale of the interaction energy, a perpendicular electric field can be applied to bias the two layers,[8,14,18–31] which causes an energy difference between the two valleys. The competition of the on-site energy difference between the layers and interactions may result in interesting physics, especially at $\nu = 0$.[14,31–35]

If the chemical potential is in the gap between Landau bands, the low-energy excitations are bound particle-hole pairs,[37–40] called magnetoexcitons .As the net charge of such an excitation is zero, taking appropriate linear combinations one obtains eigenstates of the total momentum. In such states the hole and the particle are bound by the attractive Coulomb interaction, thus form a dipole with a separation of $q\ell_B^2$ at center-of-mass wave-vector $\mathbf{q}$, where $\ell_B = \sqrt{\hbar/eB}$ is the magnetic length. These modes determine the transport gap in the $q \to \infty$ limit. Some of these modes couple to circularly polarized light,[41] while others may be observable in Raman scattering experiments.[11,42,43]

For monolayer graphene Yang *et al.*[44] studied the intra-Landau level excitations of quantum Hall ferromagnetic states, and Iyengar *et al.*[45] and Lozovik *et al.*[46] discussed the inter-Landau level excitations in detail both for the IQHE and QHF states. Infrared absorption data by Jiang *et al.*[47] and Henriksen *et al.*[48] indicate a contribution from many-body effects to the inter-Landau level transitions in these states.

In bilayer graphene Henriksen*et al.*[10] have found that fitting single-body parameters does not fully explain the observed cyclotron resonance; Deacon *et al.*[49] and Zou*et al.*[50] have found a significant particle-hole asymmetry, whose origin is still debated.[51] The wave-vector dependence of the excitations have not been observed so far. Theoretically, the intra-Landau level excitations in bilayer graphene are well understood. At odd integers in the central Landau band ($\nu = \pm 1, \pm 3$) the degeneracy of the $n = 0, 1$ Landau orbitals causes fluctuations with an in-plane electric dipole character, which gives rise to unusual collective modes.[16,52,53] At even integers in the central Landau band ($\nu = \pm 2, 0$) orbital degeneracy does not play a similar role, and the intra-level excitations are still magnetoexcitons.[34,54] To complement these studies, here we address the issue of the inter-Landau level excitations of bilayer graphene in the quantum Hall regime.

Our paper is organized as follows. In Sec. II we review the tight-binding model of bilayer graphene, and the basic facts concerning its Landau levels and orbitals. Our goal is to systematically explore the range of applicability of subsequent simplified models, which neglect several

parameters of the Slonczewski-Weiss-McClure[55] (SWM) model, or account for them on the level of perturbation theory. We intend to add a few observations to the excellent studies available in the literature.[6–8] In Sec. III we review the adaptation of the mean-field theory of magnetoexcitons to the case of bilayer graphene. In Sec. IV we study the excitations of the IQHE states, and in Sec. V those of the QHF states. We conclude in Sec. VI, with an outlook on experimental connections.

II. LANDAU LEVELS AND ORBITALS

Each layer of bilayer graphene consists of two sublattices, denoted A and B in the top layer and $\widetilde{A}$ and $\widetilde{B}$ in the bottom layer. In Bernal stacking[2] two sublattices, $\widetilde{A}$ and B in our notation, are exactly above/below one another, while the A sites are above the center of the hexagons in the bottom layer, and $\widetilde{B}$ sites are below the centers of hexagons in the top layer. See Fig. 1.

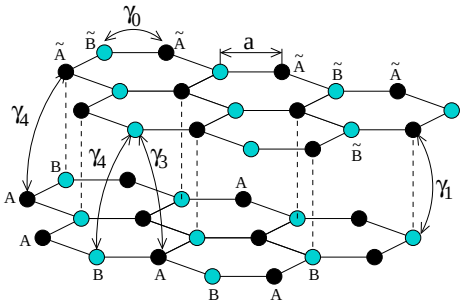

FIG. 1. (Color online) Bilayer graphene in Bernal stacking. The hopping parameters of the Slonczewski-Weiss-McClure model,[55] conventionally denoted γ_0, γ_1, γ_3 and γ_4, are also indicated.

The low-energy physics of bilayer graphene can be adequately described by the tight-binding effective theories that specialize the SWM model[55] of graphite to the case of just two layers. In the vicinity of the valley centers corresponding to the K ($\xi = 1$) and K' ($\xi = -1$) first Brillouin zone corners, this amounts to using the Hamiltonian[6]

$$\hat{H}_\xi = \xi \begin{pmatrix} \frac{u-\Delta'}{2} & v_3\pi & -v_4\pi^\dagger & v\pi^\dagger \\ v_3\pi^\dagger & -\frac{u+\Delta'}{2} & v\pi & -v_4\pi \\ -v_4\pi & v\pi^\dagger & -\frac{u-\Delta'}{2} & \xi\gamma_1 \\ v\pi & -v_4\pi^\dagger & \xi\gamma_1 & \frac{u+\Delta'}{2} \end{pmatrix} - \Delta_Z\hat{\sigma}_z, \quad (1)$$

where $\pi = p_x + ip_y$ and $\mathbf{p} = -i\hbar\nabla - e\mathbf{A}$, $v = \sqrt{3}a\gamma_0/2\hbar \approx 10^6$ m/s is the intra-layer velocity, $v_3 = \sqrt{3}a\gamma_3/2\hbar$ is the trigonal warping parameter, γ_1 is the inter-layer hopping amplitude, and $v_4 = \sqrt{3}a\gamma_4/2\hbar$ is a velocity parameter related to interlayer next-nearest neighbor hopping. $\Delta_Z = g\mu_B B_\perp$ is the Zeeman energy (with g being the gyromagnetic factor and μ_B the Bohr magneton). This Hamiltonian acts in the basis of sublattice Bloch states $[\psi_A, \psi_{\widetilde{B}}, \psi_{\widetilde{A}}, \psi_B]$ in valley K and $[\psi_{\widetilde{B}}, \psi_A, \psi_B, \psi_{\widetilde{A}}]$ in valley K'. Here $\gamma_0 = \gamma_{AB} = \gamma_{\widetilde{A}\widetilde{B}}$ is the intra-layer hopping amplitude, $\gamma_1 = \gamma_{\widetilde{A}B}$ is the interlayer hopping amplitude between sites above each other in the two layers. Further, $\gamma_3 = \gamma_{A\widetilde{B}}$ and $\gamma_4 = \gamma_{A\widetilde{A}} = \gamma_{B\widetilde{B}}$ are next-nearest neighbor interlayer hopping amplitudes, as shown in Fig. 1. Δ' is the on-site energy difference between the dimer sites $(\widetilde{A}, B)$ and the non-dimer sites $(\widetilde{B}, A)$. Finally, u is the potential energy difference between the layers, which may arise, e.g., because of an applied perpendicular electric field $E_\perp$.

The Hamiltonian in Eq. (1) is block-diagonal in the valley index, which is conveniently described as a pseudospin. In the special case $u = 0$ the system has SU(2) pseudospin rotation symmetry. In the theoretical limit $\Delta_Z \to 0$ this is raised to SU(4) symmetry. In this paper we will treat Δ_Z and u as small perturbations in comparison to the interaction energy, i.e., we will work in the $\frac{\Delta_Z}{e^2/4\pi\epsilon\ell_B} \ll 1$, $\frac{u}{e^2/4\pi\epsilon\ell_B} \ll 1$ limit. We set $\hbar = 1$.

For small momenta, $p \ll \gamma_1/4v$, the two low-energy bands of the Hamiltonian $\hat{H}_\xi$ that touch each other at K and K' in the case of vanishing magnetic field can be attributed to a 2×2 effective Hamiltonian[18]

$$\hat{H}'_\xi \approx -\frac{1}{2m}\begin{pmatrix} 0 & (\pi^\dagger)^2 \\ \pi^2 & 0 \end{pmatrix} + \xi v_3 \begin{pmatrix} 0 & \pi \\ \pi^\dagger & 0 \end{pmatrix} + \\ + \xi u \left(\frac{1}{2}\begin{pmatrix} 1 & 0 \\ 0 & -1 \end{pmatrix} - \frac{v^2}{\gamma_1^2}\begin{pmatrix} \pi^\dagger\pi & 0 \\ 0 & -\pi\pi^\dagger \end{pmatrix} \right) \quad (2)$$

where $m = \gamma_1/2v^2$, and $\hat{H}'_\xi$ acts on $[\psi_A, \psi_{\widetilde{B}}]$ in valley K and $[\psi_{\widetilde{B}}, \psi_A]$ in valley K'. The Landau levels (LL's) and Landau orbitals, respectively, of the two-band Hamiltonian $\hat{H}'_\xi$ become

$$E_{0\xi} = \frac{\xi u}{2}, \qquad E_{1\xi} = \frac{\xi u}{2} - \xi\frac{u\hbar\omega_c}{\gamma_1}, \quad (3)$$

$$E_{n\xi} = \mathrm{sgn}(n)\hbar\omega_c\sqrt{|n|(|n|-1)} - \xi\frac{u\hbar\omega_c}{2\gamma_1}, \quad (4)$$

$$\Psi_{0\text{ or }1,q} = \begin{pmatrix} \eta_{0\text{ or }1,q} \\ 0 \end{pmatrix}, \quad \Psi_{nq\xi} = \begin{pmatrix} A_\xi^{(n)}\eta_{|n|q} \\ B_\xi^{(n)}\eta_{|n|-2,q} \end{pmatrix}, \quad (5)$$

$$A_\xi^{(n)} = \frac{1}{C_\xi^{(n)}}, \quad B_\xi^{(n)} = \mathrm{sgn}(n)\left(\frac{E_{n\xi} - \xi\frac{u}{2} + \xi\frac{u|n|\hbar\omega_c}{\gamma_1}}{C_\xi^{(n)}}\right).$$

Here $n \neq -1$ is an integer, $C_\xi^{(n)}$ is an appropriate normalization factor, and η_{nq} are the single-particle states in the conventional two-dimensional electron gas with quadratic dispersion in the Landau gauge $\mathbf{A} = \hat{\mathbf{y}}Bx$,

$$\eta_{nq}(\mathbf{r}) = \frac{e^{iqx-(y/\ell_B - q\ell_B)^2/2}}{\sqrt{2\pi\sqrt{\pi}2^n n!\ell_B}} H_n\left(\frac{y}{\ell_B} - q\ell_B\right), \quad (6)$$

and H_n is a Hermite-polynomial.

The $n = 0, 1$ orbitals are degenerate in the $u \to 0$ limit, and they have a layer polarization for $\xi = \pm 1$.

At realistic values of Δ_Z and u, the $n = 0, 1$, $\xi = \pm 1$, $\sigma = \uparrow, \downarrow$ states form a quasidegenerate band we will call the central Landau level octet. Notice that $A_\xi^{(n)} \to 1/\sqrt{2}$ and $|B_\xi^{(n)}| \to 1/\sqrt{2}$ for $u \to 0$.

We would like to determine how neglecting γ_3, γ_4, and Δ' changes the single-body orbitals of $\hat{H}_\xi$ is Eq. (1), and how much these differ from the simplified two-band model $\hat{H}'_\xi$ in Eq. (2). The values of the SWM parameters for bilayer graphene was estimated by a combination of infrared response analysis and theoretical techniques by Zhang *et al.*[57] They found

$$\frac{\gamma_1}{\gamma_0} = 0.133, \quad \frac{\gamma_3}{\gamma_0} = 0.1, \quad \frac{\Delta'}{\gamma_0} = 0.006. \tag{7}$$

These ratios are based on $\gamma_0 = 3.0$ eV. While somewhat greater values of γ_0 are also available in the literature,[58] we use these values for a robustness analysis. For the particle-hole symmetry breaking term we use

$$\frac{\gamma_4}{\gamma_0} = 0.063 \tag{8}$$

from the recent electron and hole mass measurement by Zou *et al.*,[50] which is slightly greater than the value in Ref. 57.

With $\pi = \frac{\sqrt{2}\hbar}{i\ell_B} a$, $[a, a^\dagger] = 1$, the Hamiltonian can be expressed in terms of these Landau level ladder operators. Then the eigenstates of $\hat{H}_\xi$ can be calculated numerically. Fig. 2 shows the overlap of the Landau orbitals with the "ideal" limit $\gamma_3 = \gamma_4 = \Delta' = 0$ as the SWM parameters $\gamma_3, \gamma_4, \Delta'$ are tuned from zero to their literary values [Eqs. (7) to (8)] for the central ($n = 0, 1$) and the two pairs of nearby ($n = \pm 2, \pm 3$) Landau levels. At small magnetic field $B = 0.1$ T trigonal warping alone significantly changes the orbitals from their ideal limit. Switching on γ_4 hardly affects the central levels, but for $n \geq 2$ it changes the electron and hole pairs $(+n, -n)$ differently, as expected from this electron-hole symmetry breaking term. Finally, the inclusion of Δ' hardly affects the orbitals. These changes, however, are already small at modest fields ($B = 1$ T), and are further suppressed as the experimentally relevant range ($B \approx 10$ T) is approached. Thus neglecting the $\gamma_3, \gamma_4, \Delta'$ SWM parameters is justified in the high magnetic field range where quantum Hall experiments are typically performed.

As the two-band model in Eq. (2) applies for small momenta, and the low-index Landau orbitals have a small amplitude at high momenta, the two-band model is expected to be valid for the lowest few Landau levels. The Landau orbitals of the two-band model have a large overlap with those of the four-band model in the "ideal" limit $\gamma_3 = \gamma_4 = \Delta' = 0$: 1, 0.9995, 0.9992, 0.9987 for $n = 0, 1, \pm 2, \pm 3$, respectively. We conclude that using the Landau states of two-band model in Eq. (2) instead of these of the four-band model $\hat{H}_\xi$ in the lowest-energy Landau bands does not introduce further inaccuracy beyond the neglect of γ_3, γ_4 and Δ'. Therefore, we take $\hat{H}'_\xi$ as our starting point. Further, the difference between the intralayer Coulomb interaction $V^S(q) = 2\pi e^2/\epsilon q$ and the intralayer one, $V^D(q) = e^{-qd} V^S(q)$ where $d \approx 0.335$ nm is the distance between the layers, is neglected as a first approximation.

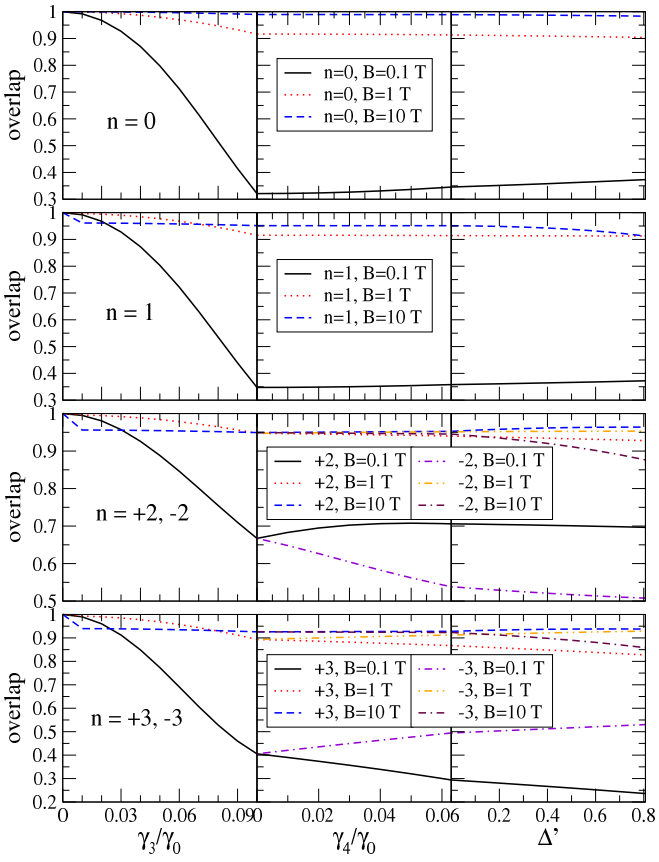

FIG. 2. (Color online) The overlap of the Landau orbitals with the "ideal" limit, $\gamma_3 = \gamma_4 = \Delta' = 0$, as the SWM parameters $\gamma_3, \gamma_4, \Delta'$ are gradually tuned from zero to their literary values [Eqs. (7) to (8)] for the lowest-energy Landau levels. For the effect of γ_3 in the two-band model see Ref. 59.

III. MAGNETOEXCITONS

When the Fermi energy is in a Landau gap (e.g. at filling factor $\nu = \ldots, -12, -8, -4, 4, 8, 12, \ldots$ in bilayer graphene), the integer quantum Hall effect[4] occurs in samples with moderate disorder.[1] Quantum Hall states also occur at other integer filling factors because the exchange interaction favors symmetry-breaking ground states called quantum Hall ferromagnets; single-body terms such as the Zeeman energy play a secondary role. QHF's emerge at odd integer fillings in two-component systems even if the Zeeman energy is tuned to zero. This observation straightforwardly generalizes for SU(n) systems.[44]

Because of the clear separation of the filled and empty Landau bands in the (mean-field) ground-state, the ex-

citations of both classes of quantum Hall systems are described in the same way. The relevant low-energy excitations are magnetoexcitons, which are obtained by promoting an electron from a filled Landau band to an empty band.[37–40] These neutral excitations have a well-defined center-of-mass momentum $\mathbf{Q}$. They approach widely separated particle-hole pairs in the $Q \to \infty$ limit. The latter limit determines the transport gap unless skyrmions form.[56] Magnetoexcitons are created from the ground-state by operators[37–40]

$$\hat{\Psi}^\dagger_{NN'}(\mathbf{Q}) = \sqrt{\frac{2\pi\ell_B^2}{A}} \sum_p e^{ipQ_y\ell_B^2} \hat{a}^\dagger_{Np}\hat{a}_{N'p-Q_x}, \qquad (9)$$

where $N = (n, \xi, \sigma)$ ($N' = (n', \xi', \sigma')$) specifies the Landau band where the particle (hole) is created and A is the area of the sample.

Magnetoexcitons carry spin and pseudospin (valley) quantum numbers, as derived from the particle and hole Landau bands involved. While the projections S_z, P_z of the spin and the pseudospin are always good quantum numbers, their magnitudes S and P are well-defined only for ground-states that are spin or pseudospin singlets, respectively.

It is common practice[37,45] to define the quantity

$$l_z = |n| - |n'|, \qquad (10)$$

and consider it the "angular momentum quantum number" of the exciton. We emphasize that l_z is exactly conserved by the electron-electron interaction only in the $\mathbf{Q} \to 0$ limit, where it is related to angular momentum. The emergence of this quantity is best seen in the two-body problem of the negatively charged electron and the positively charged hole, as discussed in the Appendix. At any finite wave vector transitions with different l_z may mix.

In the low magnetoexciton density limit the interaction between magnetoexcitons is neglected. The mean-field (Hartree-Fock) Hamiltonian of magnetoexcitons is well known from the literature,[37–40] and so is its adaptation to spinorial orbitals:[34,45]

$$H^{(\tilde{N}\tilde{N}')}_{(NN')}(\mathbf{Q}) = \langle 0|\Psi_{\tilde{N}\tilde{N}'}(\mathbf{Q})\hat{V}\Psi^\dagger_{NN'}(\mathbf{Q})|0\rangle - \delta_{N\tilde{N}}\delta_{N'\tilde{N}'}\langle 0|\hat{V}|0\rangle = \delta_{N\tilde{N}}\delta_{N'\tilde{N}'}\left(E_{n\alpha\xi\sigma} - E_{n'\alpha'\xi'\sigma'} + \Delta(n,n')\right) + E^{(\tilde{N}\tilde{N}')}_{(NN')}(\mathbf{Q}) + R^{(\tilde{N}\tilde{N}')}_{(NN')}(\mathbf{Q}), \qquad (11)$$

where $N = (n, \xi, \sigma)$, etc., and $\delta_{NN'} = \delta_{\sigma\sigma'}\delta_{\xi\xi'}\delta_{nn'}$. The first term of the r.h.s. is the single-body energy difference of the N and N' states, which includes the wave vector independent exchange self-energy difference of the two states. While the exchange self-energy itself is infinite for any orbital, its difference between two states,

$$X_{N'N} = \int \frac{d\mathbf{q}}{(2\pi)^2} I^{N'N}_{N'N}(\mathbf{p}), \qquad (12)$$

$$\Delta(N,N') = \sum_{M \text{ filled}} \left(X_{N'M} - X_{MN}\right), \qquad (13)$$

is finite. (We will define $I^{N_2N_2'}_{N_1N_1'}(\mathbf{p})$ soon.) This is a peculiarity of the two-band model of bilayer graphene, which is replaced by an appropriate renormalization procedure for monolayer graphene[45], and for the four-band model of bilayer graphene.[34]

The next term is the direct dynamical interaction between the electron and the hole:

$$E^{(\tilde{N}\tilde{N}')}_{(NN')}(\mathbf{Q}) = -\int \frac{d\mathbf{q}}{(2\pi)^2} e^{i\hat{\mathbf{z}}\cdot(\mathbf{q}\times\mathbf{Q})} I^{N\tilde{N}}_{N'\tilde{N}'}(\mathbf{q}). \qquad (14)$$

This term is diagonal both in spin and pseudospin, $\propto \delta_{\tilde{\sigma}\sigma}\delta_{\tilde{\xi}\xi}\delta_{\tilde{\sigma}'\sigma'}\delta_{\tilde{\xi}'\xi'}$, but not in Landau orbital indices. Finally, the last term in Eq. (11) is the exchange interaction between the electron and the hole,

$$R^{(\tilde{N}\tilde{N}')}_{(NN')}(\mathbf{Q}) = \frac{1}{2\pi\ell_B^2}\mathfrak{Re} I^{NN'}_{\tilde{N}\tilde{N}'}(\mathbf{Q}), \qquad (15)$$

which is $\propto \delta_{\sigma\sigma'}\delta_{\xi\xi'}\delta_{\tilde{\sigma}\tilde{\sigma}'}\delta_{\tilde{\xi}\tilde{\xi}'}$, thus couples transitions that conserve the spin σ and the valley ξ of the electron and the hole individually. Sometimes we will call it the RPA contribution, as it is related to particle-hole annihilation and recreation processes. Notice $R^{(\tilde{N}\tilde{N}')}_{(NN')}(\mathbf{Q})$ vanishes in the $Q \to 0$ limit.

We have used the notation

$$I^{N_2N_2'}_{N_1N_1'}(\mathbf{p}) = \frac{2\pi e^2}{\epsilon p}\Big[A^{(n_2')}_{\xi_2'}A^{(n_1)}_{\xi_1}A^{(n_1')}_{\xi_1'}A^{(n_2)}_{\xi_2}F^*_{|N_2||N_2'|}(\mathbf{p})F_{|N_1||N_1'|}(\mathbf{p}) + B^{(n_2')}_{\xi_2'}B^{(n_1)}_{\xi_1}B^{(n_1')}_{\xi_1'}B^{(n_2)}_{\xi_2}F^*_{|N_2|-2,|N_2'|-2,}(\mathbf{p})F_{|N_1|-2,|N_1'|-2}(\mathbf{p})\Big] + \frac{2\pi e^2}{\epsilon p}e^{-pd}\Big[A^{(n_2')}_{\xi_2'}B^{(n_1)}_{\xi_1}B^{(n_1')}_{\xi_1'}A^{(n_2)}_{\xi_2}F^*_{|N_2||N_2'|}(\mathbf{p})F_{|N_1|-2,|N_1'|-2}(\mathbf{p}) + B^{(n_2')}_{\xi_2'}A^{(n_1)}_{\xi_1}A^{(n_1')}_{\xi_1'}B^{(n_2)}_{\xi_2}F^*_{|N_2|-2,|N_2'|-2,}(\mathbf{p})F_{|N_1||N_1'|}(\mathbf{p})\Big],$$

$$F_{N'N}(\mathbf{q}) = \delta_{\sigma\sigma'}\delta_{\xi\xi'}\sqrt{\frac{n!}{(n')!}}\left(\frac{(-q_y+iq_x)\ell_B}{\sqrt{2}}\right)^{n'-n} L_n^{n'-n}\left(\frac{q^2\ell_B^2}{2}\right)e^{-q^2\ell_B^2/4} \quad \text{if } n' \geq n, \text{ else } F_{NN'}(\mathbf{q}) = F^*_{N'N}(-\mathbf{q}).$$

Here $N-2 \equiv (n-2,\xi\sigma)$, $|N| = (|n|,\xi,\sigma)$, and $F_{N'N}(\mathbf{q})$ is related to the Fourier transform of $\eta_{nq}(\mathbf{r})$ in Eq. (6), and $L_n^m(z)$ is an associated Laguerre polynomial. The $A_\xi^{(n)}$ and $B_\xi^{(n)}$ numbers correspond to the spinorial structure of the single-body states in Eq. (5): $A^1 = A^0 = 1$, $B^1 = B^0 = 0$ and $A_\xi^{(n)} = \mathrm{sgn}(n)B_\xi^{(n)} = 1/\sqrt{2}$ for $n \geq 2$. Notice that

$$(-1)^{n+n'+\tilde{n}+\tilde{n}'}E^{(\tilde{N}\tilde{N}')}_{(NN')}(\mathbf{Q}) = E^{(NN')}_{(\tilde{N}\tilde{N}')}(\mathbf{Q}) = E^{(\tilde{N}'\tilde{N})}_{(N'N)}(\mathbf{Q}), \tag{16}$$

$$R^{(\tilde{N}\tilde{N}')}_{(NN')}(\mathbf{Q}) = R^{(NN')}_{(\tilde{N}\tilde{N}')}(\mathbf{Q}) = (-1)^{n+n'+\tilde{n}+\tilde{n}'}R^{(\tilde{N}'\tilde{N})}_{(N'N)}(\mathbf{Q}), \tag{17}$$

which follow from the similar properties of $I^{N_2N_2'}_{N_1N_1'}(\mathbf{p})$.

The $q \to 0$ limit of the magnetoexciton dispersion determines the many-body contribution to the cyclotron resonance. In the case of the ordinary two-dimensional electron gas, traditionally implemented in semiconductor heterostructures and quantum wells, this mush vanish by Kohn's theorem.[60] This theorem, however, relies upon the simple quadratic form of the kinetic energy operator, thus it is not applicable in monolayer and bilayer graphene. Thus it is possible that the sum of the exchange self-energy constant $X_{NN'}$ and the diagonal part of the dynamical interaction $E^{(NN')}_{(NN')}(\mathbf{Q})$ does not vanish in the $\mathbf{Q} \to 0$ limit.

The mean field Hamiltonian matrix $H^{(\tilde{N}\tilde{N}')}_{(NN')}(\mathbf{Q})$ in general mixes transitions among different electron-hole pairs, restricted only by conservation laws. Landau level mixing effectively screens the interaction. Sometimes the magnetoexciton spectra are obtained using a screened model interaction instead of the bare Coulomb, not letting LL transitions mix.[51,59] We believe such an approach is suitable in the $q = 0$ limit, where an additional quantum number l_z also restricts LL mixing, and for intra-LL modes. At finite wave vector the mean-field theory with LL mixing removes spurious level crossings in the excitation spectra and provides insight into the orbital structure of the excitations. Technically, however, the infinite $H^{(\tilde{N}\tilde{N}')}_{(NN')}(\mathbf{Q})$ matrix needs to be truncated.

IV. INTEGER QUANTUM HALL STATES

We first consider the states where the chemical potential is between two orbital Landau bands. This occurs at filling factor $\nu = \ldots, -12, -8, -4, 4, 8, 12, \ldots$ in bilayer graphene. Together with S_z and P_z, the magnitude of the spin S and of the pseudospin P are quantum numbers. (In the $\Delta_Z \to 0, u \to 0$ limit an SU(4) classification is also possible.)

With the hole (n') and the electron (n) Landau orbitals fixed, the sixteen possible transitions belong to four classes: (i) a spin singlet, pseudospin singlet state, (ii) a spin singlet, pseudospin triplet, (iii) a spin triplet, pseudospin singlet, (iv) a nine-member multiplet that is triplet is both spin and valley. The exchange interaction between the electron and the hole contributes only to class (i), which consists of the mixture of $\{\hat{\Psi}^{\dagger 00}_{nn'}\}_{nn'}$ with

$$\hat{\Psi}^{\dagger 00}_{nn'}(\mathbf{q}) = \frac{1}{2}\sum_\xi\sum_\sigma \hat{\Psi}^\dagger_{n\sigma\xi,n'\sigma\xi}(\mathbf{q}) \tag{18}$$

In all other excitation modes the RPA term cancels or is prohibited by quantum numbers. The extent interactions may mix transitions involving different Landau level pairs depends on the interaction-to-kinetic energy ratio, parametrized by

$$\beta = \frac{e^2}{4\pi\epsilon_0\epsilon_r\ell_B}\Big/\hbar\omega_c \propto \frac{1}{\epsilon_r\sqrt{B}}, \tag{19}$$

where ϵ_r is the relative dielectric constant of the environment. LL mixing is eventually suppressed in the $B \to \infty$ limit just like for the conventional two-dimensional electron gas. Realistically ($10\ \mathrm{T} \leq B \leq 40\ \mathrm{T}$, $1 \leq \epsilon_r \leq 4$), $1 < \beta < 8$; this is by no means a small perturbation.

For $q = 0$ the mean-field Hamiltonian mixes magnetoexcitons with different electron and hole Landau levels at fixed l_z, and for $q > 0$ it also mixes different l_z subspaces. Restricting LL mixing to a fixed l_z subspace might give the impression that LL mixing is a quantitative correction for the long wave length part of the lowest excitation curves, resulting in increased electron-hole binding energy.[46,62] However, already the lowest excitations in the different l_z sectors mix strongly at finite wave length. As the side panels of Fig. 3 show, the excitations have a large projection on the l_z subspaces different from their own l_z in the $q \to 0$ limit, and are eventually contained in one of those subspaces for large q; this is an unavoidable consequence of the elimination of crossings by LL mixing. Thus in the rest of this paper we allow the mixing of transitions restricted by $|l_z| \leq L$ and a maximum number M at each fixed l_z. Fig. 3 shows transitions at $\nu = 4$ with $L = 1$ and $M = 7$, while Fig. 4 shows $|\nu| = 8$ and 12. We will use this truncation in the spectra shown in the rest of this paper.[61]

The $q \to 0$ limit of the magnetoexcitons are commonly probed by optical absorption and electronic Raman scattering. The selection rules[41,43] ensure that only the $\hat{\Psi}^{\dagger 00}_{nn'}$ mode and the three other $S_z = P_z = 0$ modes of the fifteen-fold degenerate curve are active, $l_z = \pm 1$ is absorption and $l_z = 0$ in Raman. Particle-hole conjugation

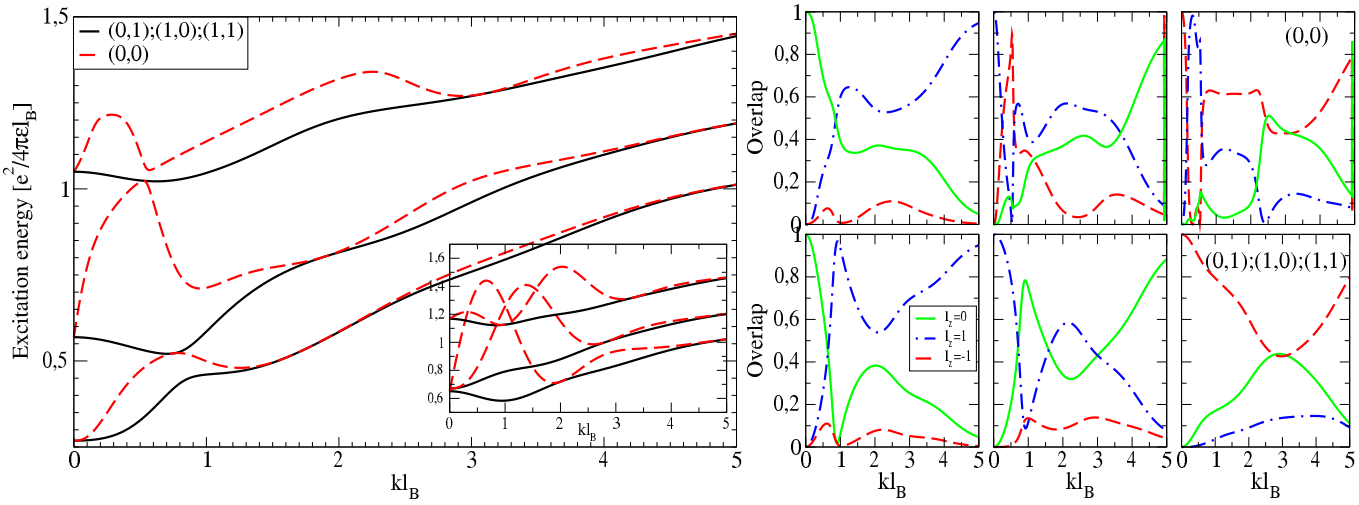

FIG. 3. (Color online) The excitations of the integer quantum Hall state at $|\nu| = 4$ and $B = 10T$. The mixing of Landau levels is truncated at $L = 1$ and $M = 7$. Solid lines show the fifteen-fold degenerate excitations, which include three optically relevant $S_z = P_z = 0$ modes. Dashed lines show the spin and pseudospin singlets. Inset: spectra if Landau level mixing is neglected. Side panels: the weight of the definite l_z projections in each curve in bottom-up order. The top row shows the spin and pseudospin singlets.

relates $\nu = 4n$ to $\nu = -4n$ (n integer) with the sign of l_z reversed.

V. QUANTUM HALL FERROMAGNETIC STATES

With an integer filling factor different from $\nu = \pm 4, \pm 8, \pm 12, \ldots$, a Landau band quartet ($|\nu| > 4$) or octet ($|\nu| < 4$) is partially filled in the single electron picture. The minimization of the interaction energy results in gapped states which break either spin rotation or pseudospin (valley) rotation symmetry, or both.[16,32,34,44,52,53,67] If either the Zeeman energy Δ_Z or the interlayer energy difference u is present, they determine the sequence how the Landau levels are filled.[16] The most convenient basis in pseudospin space may differ; we may introduce

$$\hat{a}_{nS\sigma p} = \cos\frac{\theta}{2}\hat{a}_{n,\xi=1,\sigma p} + \sin\frac{\theta}{2}e^{i\phi}\hat{a}_{n,\xi=-1,\sigma p}, \qquad (20)$$

$$\hat{a}_{nA\sigma p} = \sin\frac{\theta}{2}\hat{a}_{n,\xi=1,\sigma p} - \cos\frac{\theta}{2}e^{i\phi}\hat{a}_{n,\xi=-1,\sigma p}. \qquad (21)$$

With proper choice of θ and ϕ, these definitions include states of definite valley, bonding and antibonding states, or intervalley phase coherent states. Corresponding magnetoexciton operators are defined in an obvious manner.

In particular, if $\Delta_Z > u$, the $\nu = 0$ QHF state is ferromagnetic and the choice of the pseudospin basis is irrelevant. For $\nu = \pm 2$, both the $n = 0$ and $n = 1$ orbital Landau levels of identical pseudospin are filled, where ϕ and θ are determined by electrostatics. For odd ν, an interlayer phase coherent ($0 < \theta \leq \pi/2$) state exists

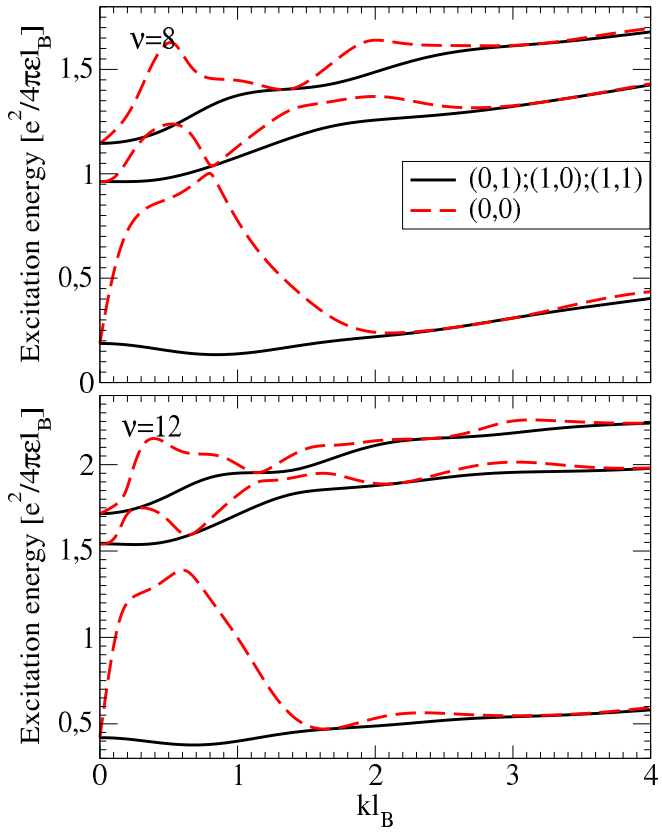

FIG. 4. (Color online) The excitations of the integer quantum Hall state at $|\nu| = 8$ and $|\nu| = 12$, at $B = 10T$.

for sufficiently small enough u, which yields[52] to a layer polarized state ($\theta = 0$) at $\nu = -3$ and $\nu = 1$, and to a sequence of states with partial or full orbital coherence[53] at $\nu = -1$ and $\nu = 3$.

Beyond S_z and P_z, the P or S are quantum numbers at half-filling $\nu = 0$. All excitons include transitions between the non-central levels $|n| \geq 2$; the possibility of transitions from, to, or within the central Landau level octet depends on the ground state, which also resolves the transitions through the exchange self-energy differences.

The excitations are grouped by their optical signature. Due to the small momenta of optical photons, valley flipping modes are optically inactive. In the $q \to 0$ limit l_z becomes a quantum number, and $l_z = \pm 1$ applies for single-photon absorption[41], and $l_z = 0, \pm 2$ in electronic Raman processes[43], with the $l_z = 0$ transitions being dominant. The angular momentum due to the helicity of the photons is transferred[41,43] entirely to the orbital degree of freedom. Optically inactive modes include Goldstone modes associated with the broken symmetry (outside the scope of our study) and generic dark modes.

A. $\nu = 0$

It is known that two QHF ground states exist, a spin-polarized one and a valley (layer) polarized one[14,16,31,32,34–36]. Their respective range of validity is determined by the ratio of the Zeeman energy Δ_Z to the energy difference between the valleys, which in turn is related to the potential difference u. (In fact, layer and pseudospin can de identified within the central Landau level octet.) For concreteness, we are discussing the ferromagnetic state. Here the magnitude of the pseudospin P is a good quantum number of the excitations.

With the electron (n) and hole (n') Landau levels fixed, the $S_z = -1$ transitions consist of a pseudospin triplet[65] $\Psi^\dagger_{nA\downarrow,n'S\uparrow}$, $\Psi^\dagger_{nS\downarrow,n'A\uparrow}$, $\frac{1}{\sqrt{2}}\left(\Psi^\dagger_{nS\downarrow,n'S\uparrow} - \Psi^\dagger_{nA\downarrow,n'A\uparrow}\right)$, and a singlet[65] $\frac{1}{\sqrt{2}}\left(\Psi^\dagger_{nS\downarrow,S\uparrow} + \Psi^\dagger_{nA\downarrow,A\uparrow}\right)$. This group contains the intralevel transitions among the $n = 0, 1$ Landau bands; the Goldstone modes associated with the spin rotational symmetry breaking should be in this subspace. However, our approach is not appropriate for the description of Goldstone modes even for even filling factors, as we will discuss below.

The $S_z = 1$ triplet and singlet of the reversed component structure, $\Psi^\dagger_{nA\uparrow,n'S\downarrow}$, $\Psi^\dagger_{nS\uparrow,n'A\downarrow}$, $\frac{1}{\sqrt{2}}\left(\Psi^\dagger_{nS\uparrow,n'S\downarrow} - \Psi^\dagger_{nA\uparrow,n'A\downarrow}\right)$, and $\frac{1}{\sqrt{2}}\left(\Psi^\dagger_{nS\uparrow,n'S\downarrow} + \Psi^\dagger_{A\uparrow,n'A\downarrow}\right)$, respectively, contains inter-LL transitions only.

The $S_z = 0$ sector consists of (i) two triplets, $\Psi^\dagger_{nA\downarrow,n'S\uparrow}$, $\Psi^\dagger_{nS\uparrow,n'A\uparrow}$, $\frac{1}{\sqrt{2}}\left(\Psi^\dagger_{nA\uparrow,n'A\uparrow} - \Psi^\dagger_{nS\uparrow,n'S\uparrow}\right)$, and $\Psi^\dagger_{nA\downarrow,n'S\downarrow}$, $\Psi^\dagger_{nS\downarrow,n'A\downarrow}$, $\frac{1}{\sqrt{2}}\left(\Psi^\dagger_{nS\downarrow,n'S\downarrow} - \Psi^\dagger_{nA\downarrow,n'A\downarrow}\right)$, the RPA terms does not contribute to, and (ii) two singlets, $\frac{1}{\sqrt{2}}\left(\Psi^\dagger_{nS\uparrow,n'S\uparrow} + \Psi^\dagger_{nA\uparrow,n'A\uparrow}\right)$ and $\frac{1}{\sqrt{2}}\left(\Psi^\dagger_{nS\downarrow,n'S\downarrow} + \Psi^\dagger_{nA\downarrow,n'A\downarrow}\right)$, which are mixed by the RPA term. Careful inspection reveals, however, that the two pseudospin singlets (ii) always appear in the mean-field Hamiltonian on equal footing, e.g., the $\frac{1}{\sqrt{2}}\left(\Psi^\dagger_{2S\uparrow,1S\uparrow} + \Psi^\dagger_{2A\uparrow,1A\uparrow}\right)$ transition is indistinguishable on the mean-field level from the $\frac{1}{\sqrt{2}}\left(\Psi^\dagger_{1S\downarrow,-2,S\downarrow} + \Psi^\dagger_{1A\downarrow,-2,A\downarrow}\right)$ transition. This follows by

$$E^{(2,1)}_{(2,1)} = E^{(1,-2)}_{(1,-2)}, \tag{22}$$

$$R^{(2,1)}_{(2,1)} = R^{(1,-2)}_{(1,-2)} = -R^{(1,-2)}_{(2,1)} = -R^{(2,1)}_{(1,-2)}, \tag{23}$$

and the following easily provable identity of the exchange self-energy cost:

$$\Delta(n,n') + X_{n'0} + X_{n'1} - X_{n,0} - X_{n,1} = \Delta(-n',-n). \tag{24}$$

(For $n = 1$ or $n' = 1$ no sign change is necessary.) Eq. (24) simply expresses particle-hole symmetry, i.e., that the exchange self-energy cost of transitions related by particle-hole conjugation in a fixed component must be identical.

The RPA terms are the same in each diagonal and off-diagonal position among equivalent transitions, thus they select the even and the odd linear combinations in group (ii). The even combination, $\hat{\Psi}^{\dagger 00}_{nn'}(\mathbf{q})$ defined in Eq. (18), gets an RPA enhancement, while the RPA cancels from the odd combination, making it energetically equivalent to the $P_z = 0$ element of the triplets (i). Thus, eventually, the $S_z = 0, P_z = 0$ sector contains a three-fold denegerate curve and a nondegenerate mode.

Each of the four multiplets in the $S_z = 0$ sector contains a $P_z = 0$ mode, which is active in electronic Raman or IR absorption.Here the mixing of Landau levels results in more widely separated modes. The optically active excitations are shown in Fig. 5 with LL mixing taken into account. Notice that the $l_z = 1$ and $l_z = -1$ transitions have an equal weight in all modes, consistent with the particle-hole symmetry at $\nu = 0$.

In the $S_z = -1$ sector we find spin waves. Neglecting Landau level mixing, they give rise to a gapless and a gapped intra-LL modes,[34] and a sequence of higher inter-LL modes; each of these is raised by the Zeeman energy and split by the valley energy difference in turn. The interaction, however, mixes these excitations, thus a clear-cut classification into intra-LL and inter-LL is no longer possible. Level repulsion unavoidably lowers the formerly gapless modes. This effect yields apparently negative excitation energies at small wavelength. Goldstone's theorem, however, ensures that a gapless spin-wave mode is associated with the breaking of the spin rotation symmetry. Consequently, the seemingly negative energies of the lowermost curves with a large intra-LL component

is an artifact of the combination of Hartree-Fock mean-field theory and LL mixing. The same anomaly occurs for monolayer graphene[45,46], but it is less apparent when the particle-hole binding energy is plotted.

B. $\nu = \pm 2$

The $\nu = \pm 2$ state breaks the spin and pseudospin rotational symmetries as the ground state fills the $n = 0$ and $n = 1$ orbitals of the most favorable spin-pseudospin component, $S\uparrow$. We restrict the discussion to spin and pseudospin preserving excitations. It is easy to check that the mean-field Hamiltonian matrix is identical to the one at $\nu = 0$. For the $-n \to n$ transitions ($n \geq 2$ integer) this holds because the occupancy of the central Landau level octet is irrelevant as

$$X_{-n,0} + X_{-n,1} - X_{n,0} - X_{n,1} = 0. \tag{25}$$

The octet of $-(n+1) \to n$ and $-n \to (n+1)$ transitions gives rise to two quartets of equivalent transitions by Eqs. (22-24). While at $\nu = 0$ the $S\uparrow$ and $A\uparrow$ transitions of the former group bundle with the $S\downarrow$ and $A\downarrow$ transitions of the second group, now the $S\uparrow$ transition of the first group bundle with the $A\uparrow$, $S\downarrow$ and $A\downarrow$ transitions of the second group. The spectra is still the one in Fig. 5(a). The orbital projection of the modes differs, c.f. Fig. 6 for $\nu = -2$. At $\nu = +2$ the sign of l_z changes in all projections, which determines the helicity of the absorbed and inelastically scattered photons.

C. $\nu = -3$

At $\nu = -3$ the only occupied band is $(0, S\uparrow)$. The $n = 0$ orbitals are selected by their small energetic advantage. The states in Eq. (20) progress from the layer balanced limit $\theta = \pi$ at $u = 0$ to the layer polarized state $\theta = 0$; this limit is achieved about $u = u_c \approx 0.001 e^2/\epsilon\ell_B$, which is only 0.082 meV at $B = 20$ T. For $0 < u < u_c$ there is interlayer phase coherence.[52] Thus magnetoexcitons exist on both side of u_c; the amount electrostatics raises energy of the pseudospin-flipping modes w.r.t. the pseudospin conserving modes saturates at $u = u_c$. Both the spin and the pseudospin symmetries are broken resulting in a three-fold Goldstone mode.[52] Further, Barlas *et al.*[52] showed that at finite u there is an instability to a stripe ordered phase with a rather small critical temperature. Our analysis below applies only below this temperature.

Notice that $\nu = -3$ and $\nu = 3$ are not related by particle-hole symmetry. This is best understood from Hund's rules[16]: at $\nu = -3$ only one $n = 0$ orbital band is occupied, while at $\nu = 3$ only one $n = 1$ orbital band is empty. At $\nu = 3$ Côté *et al.*[53] showed that orbitally coherent states dominate the phase diagram, whose inter-LL excitations are beyond the scope of this study.

Because of the degeneracy of $n = 0, 1$ orbitals, states in central Landau level octet at odd integer fillings involve fluctuations with in-plane electric dipole character.[16] The consequent collective modes have been studied in detail by Barlas *et al.*[52] and Côte *et al.*[53] As we do not handle such dipolar interactions, we have omitted the predominantly intra-LL lowest curve from the spectra, and we have checked that the inter-LL excitation modes we keep contain the $0 \to 1$ magnetoexcitons with a negligible weight. Reassuringly, we always got a weight less than 0.1%.

As the $n = 0$ orbital is filled with $S\uparrow$ electrons in the mean-field ground state, the self-energy cost of $S\uparrow$ transitions is higher than those of the other component with identical electron and hole Landau orbitals. Also, in the $S\uparrow$ component an intralevel $0 \to 1$ transition is possible, which mixes with higher $S\uparrow$ transitions. The other three components, on the other hand, occur symmetrically in the mean-field Hamiltonian. This follows as in the case of $\nu = \pm 2$. One can change basis from the excitons of type $S\downarrow$, $A\uparrow$ and $A\downarrow$ to

$$\hat{\Psi}^{\dagger d1}_{nn'} = \frac{1}{\sqrt{2}} \left(\Psi^\dagger_{nA\uparrow,n'A\uparrow} - \Psi^\dagger_{nA\downarrow,n'A\downarrow} \right), \tag{26}$$

$$\hat{\Psi}^{\dagger d2}_{nn'} = \frac{1}{\sqrt{6}} \left(\Psi^\dagger_{nA\uparrow,n'A\uparrow} + \Psi^\dagger_{nA\downarrow,n'A\downarrow} - 2\Psi^\dagger_{nS\downarrow,n'S\downarrow} \right), \tag{27}$$

$$\hat{\Psi}^{\dagger r}_{nn'} = \frac{1}{\sqrt{3}} \left(\Psi^\dagger_{nA\uparrow,n'A\uparrow} + \Psi^\dagger_{nA\downarrow,n'A\downarrow} + \Psi^\dagger_{nS\downarrow,n'S\downarrow} \right). \tag{28}$$

The RPA contribution cancels from $\hat{\Psi}^{\dagger d1}_{nn'}(\mathbf{q})$ and $\hat{\Psi}^{\dagger d2}_{nn'}(\mathbf{q})$, which give rise to doubly degenerate excitations. $\hat{\Psi}^{\dagger r}_{nn'}(\mathbf{q})$ has an RPA contribution. Its mixture with the distinguished $S\uparrow$ excitations produces singlet excitations. In higher energy excitations, on the other hand, the weight of the $0 \to 1$ transition of the $S\uparrow$ component becomes extremely small, thus the equivalence of components will be approximately restored, yielding threefold quasi-degenerate and nondegenerate curves.

See Fig. 7 for the dispersion of the active excitations. The small graphs show that the projection to definite l_z subspaces changes abruptly at nonzero wave vector.

D. $\nu = 1$

Just like at $|\nu| = 3$, the states at $\nu = -1$ is not the particle-hole conjugate of the state $\nu = 1$. We do not study $\nu = -1$ because of the revelance or orbitally coherent states[72]. At $\nu = 1$ the interlayer coherent and layer polarized QHF states both have magnetoexcitons.

The $S\downarrow$ electrons are distinguished by their higher self-energy cost and the possibility of an intralevel $0 \to 1$ transition. The other three components occur symmetrically in the mean-field Hamiltonian. The argument is similar to the case of $\nu = \pm 2$ and $\nu = -3$; for the two $1 \to 2$ transitions of spin-$\uparrow$ electrons and the $-2 \to 1$ transitions of the spin-$\downarrow$ electrons one uses $R^{(2,1)}_{(1,0)} = -R^{(1,-2)}_{(1,0)}$

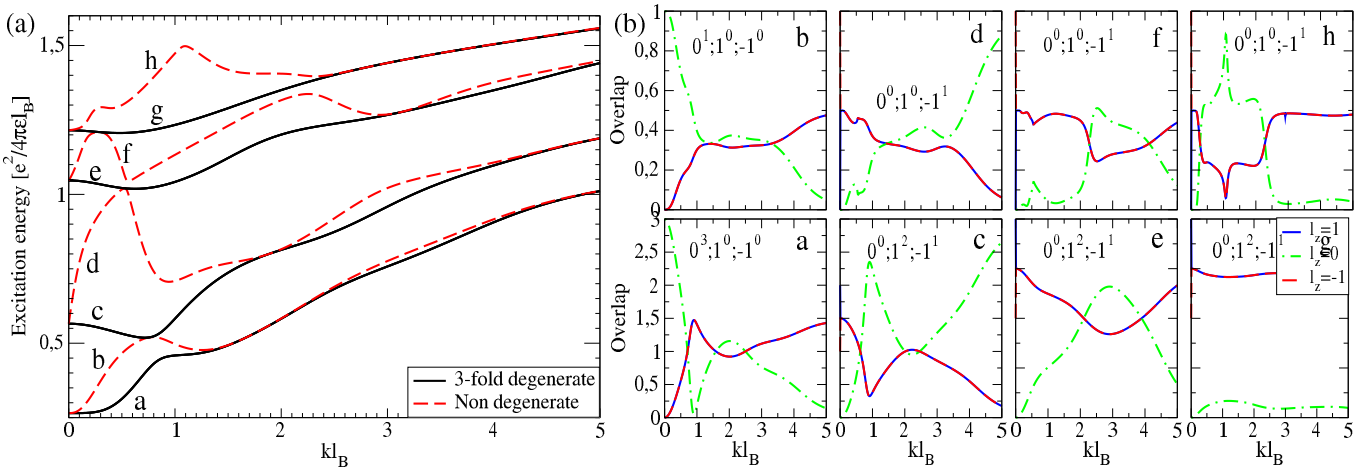

FIG. 5. (Color online) (a) Excitation spectra of the quantum Hall ferromagnet at $\nu = 0, \pm 2$ at $B = 10$ T. Only the optically relevant $S_z = P_z = 0$ modes are included. (b) The weight of the shown excitations on the definite l_z subspaces for $\nu = 0$ in bottom-up order. For degenerate curves the weight is summed. The quantum numbers of the $q \to 0$ limit are indicated.

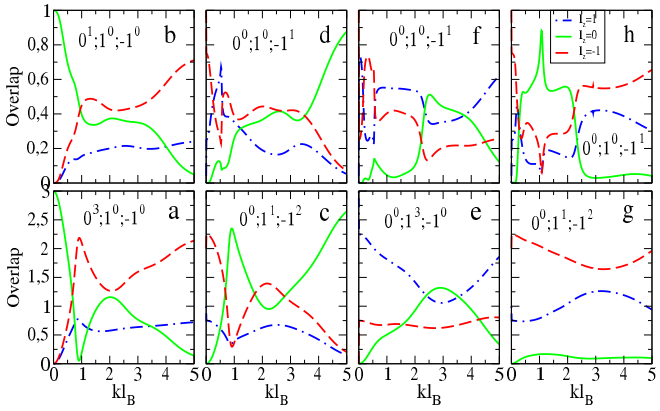

FIG. 6. (Color online) The projection of the excitations at $\nu = -2$ on the definite l_z subspaces. For degenerate curves the weight is summed. The spectrum at $\nu = \pm 2$ is identical to the one in the left panel of Fig. 5, the letters refer to the same curves. For $\nu = +2$ the sign of the $+l_z$ and $-l_z$ projections are interchanged w.r.t. $\nu = -2$.

and Eq. (24). When subsequent $l_z = \pm 1$ transitions are included, the $-n \to (n+1)$ transition of $A\downarrow$ is equivalent to the $-(n+1) \to n$ transition of $S\uparrow$ and $A\uparrow$, while the $-n \to (n+1)$ transition of $A\uparrow$ and $S\uparrow$ is equivalent to the $-(n+1) \to n$ transition of $A\downarrow$. The convenient basis change is similar to Eqs. (26) to (28), with $S\uparrow$ replaced by $A\downarrow$. In fact, there is only a slight difference between the inter-level excitation spectra at $\nu = -3$ and $\nu = 1$: the exchange self-energy cost of the distinguished transition ($S\uparrow$ at $\nu = -3$ and $S\downarrow$ at $\nu = 1$) relative to the three equivalent ones is $X_{n'0} - X_{n0}$ at $\nu = -3$ and $X_{n'1} - X_{n1}$ at $\nu = 1$. The spectra are shown in Fig. 7.

VI. CONCLUSION

We have calculated the inter-Landau level magnetoexcitons in the integer quantum Hall states as wells as the quantum Hall ferromagnets at filling factor $\nu = -3, \pm 2, 0, 1$ of bilayer graphene. We have found that the spinorial structure of the orbitals together with the enhanced electron-hole exchange interaction effects in this multicomponent system gives rise to rather complex dispersions, which should be observable in inelastic photon scattering. The mixing of transitions that involve different Landau levels is strong in the experimentally accessible range. This mixing smoothens the dispersion relations via level repulsion, and at finite wavelength causes a strong mixing of the modes that have distinct angular momenta in the zero wavevector limit.

ACKNOWLEDGEMENTS

C. T. was supported by the SROP-4.2.2/08/1/2008-0011 and SROP-4.2.1.B-10/2/KONV-2010-0002 grants, and the Bolyai Fellowship of the Hungarian Academy of Sciences.

Appendix A: The two-body problem in bilayer graphene

Let us consider the Hamiltonian

$$\hat{H}_2 = -\frac{1}{2m}\begin{pmatrix} 0 & (\pi_1^\dagger)^2 \\ \pi_1^2 & 0 \end{pmatrix} - \frac{1}{2m}\begin{pmatrix} 0 & (\pi_2^\dagger)^2 \\ \pi_2^2 & 0 \end{pmatrix} - u(\mathbf{r}_1 - \mathbf{r}_2), \tag{A1}$$

where $\pi_i = p_{i,x} + ip_{i,y}$, $\mathbf{p}_1 = -i\hbar\nabla_1 - (e/c)\mathbf{A}(\mathbf{r}_1)$ belongs to the electron and $\mathbf{p}_2 = -i\hbar\nabla_2 + (e/c)\mathbf{A}(\mathbf{r}_2)$ belongs to

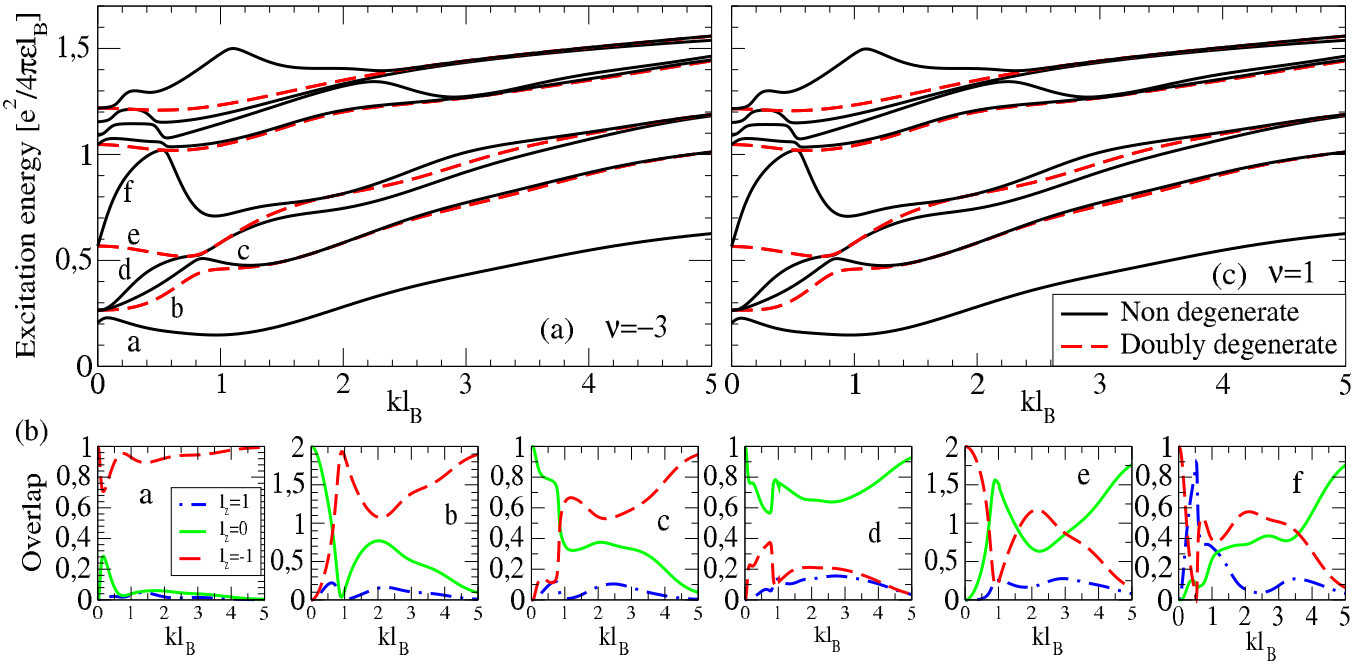

FIG. 7. (Color online) (a) Excitation spectrum of the quantum Hall ferromagnet in the $\nu = -3$ and $\nu = 1$ at $B = 10$ T. Only the optically relevant $S_z = P_z = 0$ modes are included. (b) The weight of the shown excitations on the definite l_z subspaces in bottom-up order. For degenerate curves the weight is summed. (c) Spectrum at $\nu = 1$, same parameters.

the hole, and $u(\mathbf{r}) = e^2/\epsilon r$. (We have fixed the valley of both the electron and the hole. A valley-independent interaction is assumed because any deviation from this is small in the ratio of the lattice constant to the magnetic length.) Introducing center-of-mass and relative coordinates $(X, Y) = \frac{\mathbf{r}_1+\mathbf{r}_2}{2}$, $(x, y) = \mathbf{r}_1 - \mathbf{r}_2$ and momenta $(P_x, P_y) = \mathbf{r}_1 + \mathbf{r}_2$, $(p_x, p_y) = \frac{\mathbf{p}_1+\mathbf{p}_2}{2}$, and separating the center-of-mass motion by the canonical transformation $\hat{U} = e^{iXy}$, we obtain

$$\hat{H}_2' = -\frac{1}{m}\begin{pmatrix} 0 & C_-^2 & (C_+^\dagger)^2 & 0 \\ (C_-^\dagger)^2 & 0 & 0 & (C_+^\dagger)^2 \\ C_+^2 & 0 & 0 & C_-^2 \\ 0 & C_+^2 & (C_-^\dagger)^2 & 0 \end{pmatrix} - u(\mathbf{r}-\hat{\mathbf{z}}\times\mathbf{P}), \tag{A2}$$

where the independent harmonic oscillators $C_\pm$ are defined as

$$C_\pm = \frac{(p_x - i\frac{x}{2}) \pm i(p_y - i\frac{y}{2})}{2\sqrt{2}}. \tag{A3}$$

In complete analogy to the case of the monolayer[45], the eigenstates of the kinetic part of $\hat{H}_2'$ are

$$\Psi_{n_+,n_-} \propto \begin{pmatrix} S(n_-)\phi_{|n_+|,|n_-|-2} \\ \phi_{|n_+|,|n_-|} \\ S(n_+)S(n_-)\phi_{|n_+|-2,|n_-|-2} \\ S(n_+)\phi_{|n_+|-2,|n_-|} \end{pmatrix}, \tag{A4}$$

in terms of two-dimensional harmonic oscillator eigenstates,

$$\phi_{nm}(\mathbf{r}) = \frac{(C_+^\dagger)_\xi^{(n)}}{\sqrt{n!}}\frac{(C_-^\dagger)^m}{\sqrt{m!}}\frac{1}{\sqrt{2\pi}\ell_B}e^{-r^2/4\ell_B^2}. \tag{A5}$$

Above $S(n) = 0$ is if $n = 0$ or $n = 1$, else it is $\mathrm{sgn}(n)$. Thus the kinetic energy operator clearly commutes with the operator

$$\hat{L} = C_+^\dagger C_+ - C_-^\dagger C_- + \begin{pmatrix} -2 & 0 & 0 & 0 \\ 0 & 0 & 0 & 0 \\ 0 & 0 & 0 & 0 \\ 0 & 0 & 0 & 2 \end{pmatrix},$$

which returns l_z as an eigenvalue. This operator, however, commutes with the complete $\hat{H}_2'$ only in the $\mathbf{P} \to 0$ limit. Thus we can regard the electron-hole bound state as a two-dimensional harmonic oscillator with clockwise (C_+) and anti-clockwise (C_-) excitations placed in an external confinement potential. A nonzero center-of-mass motion breaks the rotational symmetry of this confinement and starts to couple the Ψ_{n_+,n_-} states.

Here we closely follow Iyengar *et al.*[45] The two-body Hamiltonian in Eq. (A1) can be written is terms of center-

of-mass and relative coordinates and momenta as

$$\begin{aligned}\hat{H}_2 =& -\frac{m_x^+}{2m}\left(\frac{P_x^2}{2}+2p_x^2-\frac{(P_y-x)^2}{2}-2(p_y-X)^2\right)\\ &-\frac{m_x^-}{2m}\left(2P_xp_x-2(p_y-X)(P_y-x)\right)\\ &+\frac{m_y^+}{2m}\left(P_x(P_y-x)+2p_x(p_y-X)\right)\\ &+\frac{m_y^-}{2m}\left(P_x(p_y-X)+(p_y-X)P_x+\right.\\ &\left.+p_x(Py-x)+(P_y-x)p_x\right)-u(\mathbf{r}),\end{aligned}\tag{A6}$$

where $m_x^\pm=\frac{1}{2}(\sigma_x\otimes 1\pm 1\otimes\sigma_x)$, and $m_y^\pm=-\frac{1}{2}(\sigma_y\otimes 1\pm 1\otimes\sigma_y)$. With the application of the canonical transformation $\hat{U}=e^{iXy}$, we obtain

$$\begin{aligned}\hat{H}_2' =& -\frac{m_x^+}{2m}\left(\frac{y^2}{2}+2{p_x'}^2-\frac{x^2}{2}-2{p_y'}^2\right)\\ &-\frac{m_x^-}{2m}\left(2yp_x'-2p_y'x\right)\\ &-\frac{m_y^+}{2m}\left(yx-4p_x'p_y'\right)\\ &-\frac{m_y^-}{2m}\left(-yp_y'-p_y'y+p_x'x+xp_x'\right)\\ &-u(\mathbf{r}-\hat{\mathbf{z}}\times\mathbf{P}').\end{aligned}\tag{A7}$$

Eq. (A2) follows by substituting Eq. (A3) into Eq. (A7). Notice that $\hat{H}_2'$ in Eq. (A2) is independent of the transformed center-of-mass coordinates. Thus $\mathbf{P}'$ is conserved; in original variables this corresponds to $\mathbf{P}-e\mathbf{r}\times\mathbf{B}$.

[1] K. S. Novoselov, E. McCann, S. V. Morozov, V. I. Falko, M. I. Katsnelson, U. Zeitler, D. Jiang, F. Schedin, and A. K. Geim, Nat. Phys. **2**, 177 (2006).
[2] J. D. Bernal, Proc. Roy. Soc. A **106**, 749 (1924).
[3] V. I. Fal'ko, Phil. Trans. R. Soc. A **366**, 205 (2008).
[4] K. von Klitzing, G. Dorda, and M. Pepper, Phys. Rev. Lett. **45**, 494 (1980).
[5] V. I. Fal'ko, Phil. Trans. R. Soc. A **366**, 205 (2008).
[6] E. McCann and V. I. Fal'ko, Phys. Rev. Lett. **96**, 086805 (2006); F. Guinea, A. H. Castro Neto, N. M. R. Peres, Phys. Rev. B **73**, 245426 (2006);
[7] J. M. Pereira, Jr., F. M. Peeters, and P. Vasilopoulos, Phys. Rev. B **76**, 115419 (2007).
[8] L. M. Zhang, M. M. Fogler, and D. P. Arovas, Phys. Rev. B **84**, 075451 (2011).
[9] E. V. Kurganova, A. J. M. Giesbers, R. V. Gorbachev, A. K. Geim, K. S. Novoselov, J. C. Maan, U. Zeitler, Solid State Commun. **150**, 2209 (2010).
[10] E. A. Henriksen, Z. Jiang, L.-C. Tung, M. E. Schwartz, M. Takita, Y.-J. Wang, P. Kim, H. L. Stormer, Phys. Rev. Lett. **100**, 087403 (2008).
[11] C. Faugeras, M. Amado, P. Kossacki, M. Orlita, M. Kühne, A. A. L. Nicolet, Yu. I. Latyshev, and M. Potemski, Phys. Rev. Lett. **107**, 036807 (2011).
[12] B. E. Feldman, J. Martin, and A. Yacoby, Nature Physics **5**, 889 (2009).
[13] Y. Zhao, P. Cadden-Zimansky, Z. Jiang, and P. Kim, Phys. Rev. Lett. **104**, 066801 (2010).
[14] R. T. Weitz, M. T. Allen, B. E. Feldman, J. Martin, and A. Yacoby, Science **330**, 812 (2010).
[15] H. J. van Elferen, A. Veligura, E. V. Kurganova, U. Zeitler, J. C. Maan, N. Tombros, I. J. Vera-Marun, and B. J. van Wees, Phys. Rev. B **85**, 115408 (2012).
[16] Y. Barlas, R. Côté, K. Nomura, and A. H. MacDonald, Phys. Rev. Lett. **101**, 097601 (2008).
[17] W. Bao, Z. Zhao, H. Zhang, G. Liu, P. Kratz, L. Jing, J. Velasco, Jr., D. Smirnov, and C. N. Lau, Phys. Rev. Lett. **105**, 246601 (2010).
[18] E. McCann, Phys. Rev B **74**, 161403 (2006).
[19] T. Ohta, A. Bostwick, T. Seyller, K. Horn, and E. Rotenberg, Science **313**, 951 (2006).
[20] E. V. Castro, K. S. Novoselov, S. V. Morozov, N. M. R. Peres, J. M. B. Lopes dos Santos, J. Nilsson, F. Guinea, A. K. Geim, and A. H. Castro Neto, Phys. Rev. Lett. **99**, 216802 (2007).
[21] H. Min, B. Sahu, S. K. Banerjee, and A. H. MacDonald, Phys. Rev. B **75**, 155115 (2007).
[22] J. B. Oostinga, H. B. Heersche, X. Liu, A. F. Morpurgo, and L. M. K. Vandersypen, Nat. Mat. **7**, 151 (2007) .
[23] A. B. Kuzmenko, E. van Heumen, D. van der Marel, P. Lerch, P. Blake, K. S. Novoselov, and A. K. Geim, Phys. Rev. B **79**, 115441 (2009).
[24] Y. Zhang, T.-T. Tang, C. Girit, Z. Hao, M. C. Martin, A. Zettl, M. F. Crommie, Y. R. Shen, and F. Wang, Nature **459**, 820 (2009).
[25] K. F. Mak, C. H. Lui, J. Shan, T. F. Heinz, Phys. Rev. Lett. **102**, 256405 (2009).
[26] M. Mucha-Kruczyński, E. McCann, V.I. Fal'ko, Solid State

Commun. **149**, 1111 (2009).
[27] D. Wang and G. Jin, Europhys. Lett. **92**, 57008 (2010).
[28] J. B. Oostinga, H. B. Heersche, X. Liu, A. F. Morpurgo, and L. M. K. Vandersypen, Nat. Mat. **7**, 151 (2007).
[29] Y. Zhang, T.-T. Tang, C. Girit, Z. Hao, M. C. Martin, A. Zettl, M. F. Crommie, Y. R. Shen, and F. Wang, Nature **459**, 820 (2009).
[30] J. Yan and M. S. Fuhrer, Nano Lett. **10**, 4521 (2010).
[31] S. Kim and E. Tutuc, arXiv:0909.2288 (2009).
[32] E. V. Gorbar, V. P. Gusynin, and V. A. Miransky, JETP Lett. **91**, 314 (2010); Phys. Rev. B **81**, 155451 (2010); E. V. Gorbar, V. P. Gusynin, V. A. Miransky, and I. A. Shovkovy, Phys. Rev. B **85**, 235460 (2012) (2012).
[33] R. Nandkishore and L. Levitov, Phys. Rev. Lett. **104**, 156803 (2010); A relevant discussion is only avalable in a previous version of this paper, arXiv:0907.5395v1 (2009),
[34] C. Tőke and V. I. Fal'ko, Phys. Rev. B **83**, 115455 (2011).
[35] M. Kharitonov, Phys. Rev. Lett. **109**, 046803 (2012).
[36] At certain values of the in-plane pseudospin anisotropy, which may arise due to electron-electron and electron-phonon interactions, two more phases are possible: a canted antiferromagnet and a partially layer polarized state, c.f. Ref. 35. These recently proposed states are beyond the scope of our study.
[37] C. Kallin and B. I. Halperin, Phys. Rev. B **30**, 5655 (1984).
[38] A. H. MacDonald, J. Phys. C: Solid State Phys. **18**, 1003 (1985).
[39] I. V. Lerner and Yu. E. Lozovik, Zh. Eksp. Teor. Fiz. **78**, 1167 (1980) [Sov. Phys. JETP **51**, 588 (1981)].
[40] Yu. A. Bychkov, S. V. Iordanskii, and G. M. Eliashberg, Pis'ma Zh. Eksp. Teor. Fiz. **33**, 152 (1981) [Sov. Phys. JETP Lett. **33**, 143 (1981)]; Yu. A. Bychkov, E. I. Rashba, Zh. Eksp. Teor. Fiz. **85**, 1826 (1980) [Sov. Phys. JETP **58**, 1062 (1983)].
[41] D. S. L. Abergel and V. I. Fal'ko, Phys. Rev. B **75**, 155430 (2007).
[42] A. Pinczuk, B. S. Dennis, L. N. Pfeiffer, K. W. West, Semicond. Sci. Technol. **9**, 1865 (1994).
[43] M. Mucha-Kruczyński, O. Kashuba, and V. I. Fal'ko, Phys. Rev. B **82**, 045405 (2010).
[44] K. Yang, S. Das Sarma, A. H. MacDonald, Phys. Rev. B **74**, 075423 (2006).
[45] A. Iyengar, J. Wang, H. A. Fertig, and L. Brey, Phys. Rev. B **75**, 125430 (2007).
[46] Yu. E. Lozovik and A. A. Sokolik, Nanoscale Res. Lett. **7**, 134 (2012).
[47] Z. Jiang, E. A. Henriksen, L. C. Tung, Y.-J. Wang, M. E. Schwartz, M. Y. Han, P. Kim, and H. L. Stormer, Phys. Rev. Lett. **98**, 197403 (2007).
[48] E. A. Henriksen, P. Cadden-Zimansky, Z. Jiang, Z. Q. Li, L.-C. Tung, M. E. Schwartz, M. Takita, Y.-J. Wang, P. Kim, H. L. Stormer, Phys. Rev. Lett. **104**, 067404 (2010).
[49] R. S. Deacon, K.-C. Chuang, R. J. Nicholas, K. S. Novoselov, and A. K. Geim, Phys. Rev. B **76**, 081406(R) (2007).
[50] K. Zou, X. Hong, J. Zhu, Phys. Rev. B **84**, 085408 (2011).
[51] K. Shizuya, Phys. Rev. B **81**, 075407 (2010).
[52] Y. Barlas, R. Côté, J. Lambert, A. H. MacDonald, Phys. Rev. Lett. **104** 096802 (2010).
[53] R. Côté, J. Lambert, Y. Barlas, and A. H. MacDonald, Phys. Rev. B **82**, 035445 (2010).
[54] K. Shizuya, Phys. Rev. B **79**, 165402 (2009).
[55] P. R. Wallace, Phys. Rev. **71**, 622 (1947); J. W. McClure, Phys. Rev. **108**, 612 (1957); J. C. Slonczewski and P. R. Weiss, Phys. Rev. **109**, 272 (1958).
[56] S. L. Sondhi, A. Karlhede, S. A. Kivelson, and E. H. Rezayi, Phys. Rev. B **47**, 16419 (1993); H. A. Fertig, L. Brey, R. Côté, A. H. MacDonald, A. Karlhede, and S. L. Sondhi, Phys. Rev. B **55**, 10671 (1997).
[57] L. M. Zhang, Z. Q. Li, D. N. Basov, M. M. Fogler, Z. Hao and M. C. Martin, Phys. Rev. B **78**, 235408 (2008).
[58] Z. Q. Li, E. A. Henriksen, Z. Jiang, Z. Hao, M. C. Martin, P. Kim, H. L. Stormer, and D. N. Basov, Phys. Rev. Lett. **102**, 037403 (2009).
[59] T. Misumi and K. Shizuya, Phys. Rev. B **77**, 195423 (2008).
[60] W. Kohn, Phys. Rev. **123**, 1242 (1961).
[61] At $q = 0$ we have attempted an extrapolation of the excitation energies as a function of the cutoff M. The energies show a decreasing tendency, but fitting a power function[46] has proved to be impossible. We have chosen an ad-hoc cutoff at $M = 7$, with the understanding that small quantitative deviations are possible, especially at low energies.
[62] S. A. Moskalenko, M. A. Liberman, P. I. Khadzhi, E. V. Dumanov, I. V. Podlesny, and V. Botan, Solid State Commun. **140**, 236 (1996); Physica E **39**, 137 (2007).
[63] J. G. Checkelsky, L. Li, and N. P. Ong, Phys. Rev. Lett. **100**, 206801 (2008); Phys. Rev. B **79**, 115434 (2009).
[64] G. M. Gusev, E. B. Olshanetsky, Z. D. Kvon, N. N. Mikhailov, S. A. Dvoretsky, and J. C. Portal, Phys. Rev. Lett. **104**, 166401 (2010).
[65] One can easily check that the equal sign linear combination of the excitons created by the operators $(S\downarrow, S\uparrow)$ and $(A\downarrow, A\uparrow)$ is a pseudospin singlet, whereas the opposite sign linear combination is a member of a pseudospin triplet: Compare $P_-\hat{\Psi}^\dagger_{n\uparrow S,n'\uparrow S}|\mathrm{gs}\rangle$ with $\left(\Psi^\dagger_{n\uparrow S,n'\downarrow S} \pm \Psi^\dagger_{n\uparrow A,n'\downarrow A}\right)|\mathrm{gs}\rangle$, where P_- is the total pseudospin lowering operator and $|\mathrm{gs}\rangle$ is a ground state that is invariant for pseudospin rotation.
[66] A. M. Fischer, A. B. Dzyubenko, and R. A. Roemer, Phys. Rev. B **80**, 165410 (2009).
[67] V. E. Bisti and N. N. Kirova, Phys. Rev. B **84**, 155434 (2011).
[68] Y. H. Lai, J. H. Ho, C. P. Chang, and M. F. Lin, Phys. Rev. B **77**, 085426 (2008).
[69] J. Martin, B. E. Feldman, R. T. Weitz, M. T. Allen, and A. Yacoby, Phys. Rev. Lett. **105**, 256806 (2010).
[70] S. Kim, K. Lee, and E. Tutuc, Phys. Rev. Lett. **107**, 016803 (2011).
[71] C. R. Dean, A. F. Young, I. Meric, C. Lee, L. Wang, S. Sorgenfrei, K. Watanabe, T. Taniguchi, P. Kim, K. L. Shepard, and J. Hone, Nat. Nanotech. **5**, 722 (2010).
[72] Y. Barlas, W.-Ch. Lee, K. Nomura, and A. H. MacDonald, Int. J. Mod. Phys. B **23**, 2634 (2009).
[73] W. Bao, J. Velasco Jr, F. Zhang, L. Jing, B. Standley, D. Smirnov, M. Bockrath, A. H. MacDonald, and C. N. Lau, Proc. Nat. Acad. Sci. **109**, 10802 (2012).